SUPPLEMENTAL INVENTORY

Fig. S1 and Table S1 are related to Fig. 1.

Table S2 is related to Fig. 2.

Fig. S2 is related to Fig. 3.

Fig. S3 is related to Fig. 5.

Movie S1 is related to Fig. 6.

Fig. S4 is related to Fig. 7.

Fig. S1

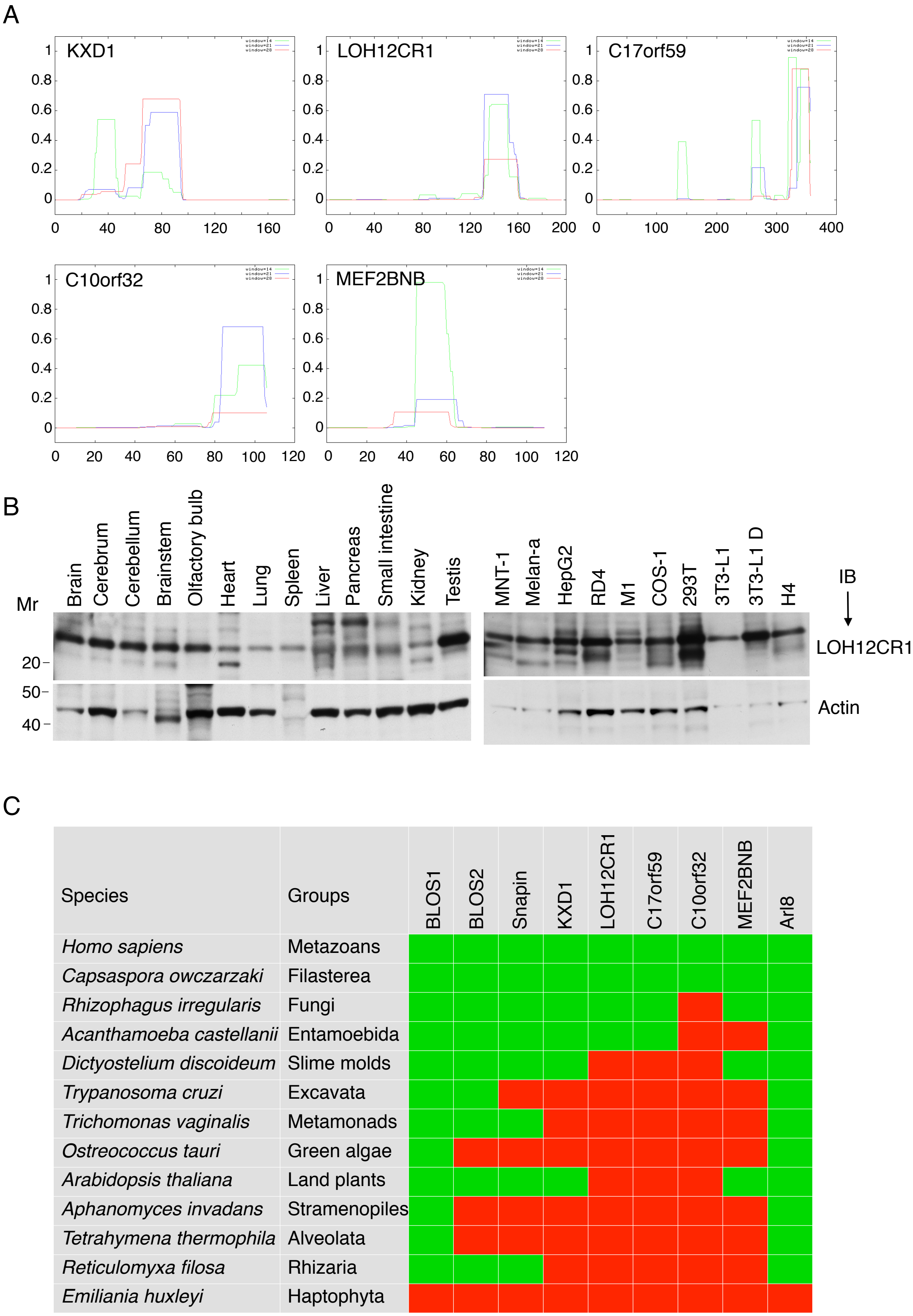
A
KXD1
LOH12CR1
C17orf59
C10orf32
MEF2BNB
B
Brain
Cerebrum
Cerebellum
Brainstem
Olfactory bulb
Heart
Lung
Spleen
Liver
Pancreas
Small intestine
Kidney
Testis
MNT-1
Melan-a
HepG2
RD4
M1
COS-1
293T
3T3-L1
3T3-L1 D
H4
IB
Mr
20
50
40
LOH12CR1
Actin
C
Species
Groups
BLOS1
BLOS2
Snapin
KXD1
LOH12CR1
C17orf59
C10orf32
MEF2BNB
Arl8
Homo sapiens
Metazoans
Capsaspora owczarzaki
Filasterea
Rhizophagus irregularis
Fungi
Acanthamoeba castellanii
Entamoebida
Dictyostelium discoideum
Slime molds
Trypanosoma cruzi
Excavata
Trichomonas vaginalis
Metamonads
Ostreococcus tauri
Green algae
Arabidopsis thaliana
Land plants
Aphanomyces invadans
Stramenopiles
Tetrahymena thermophila
Alveolata
Reticulomyxa filosa
Rhizaria
Emiliania huxleyi
Haptophyta

Fig. S2

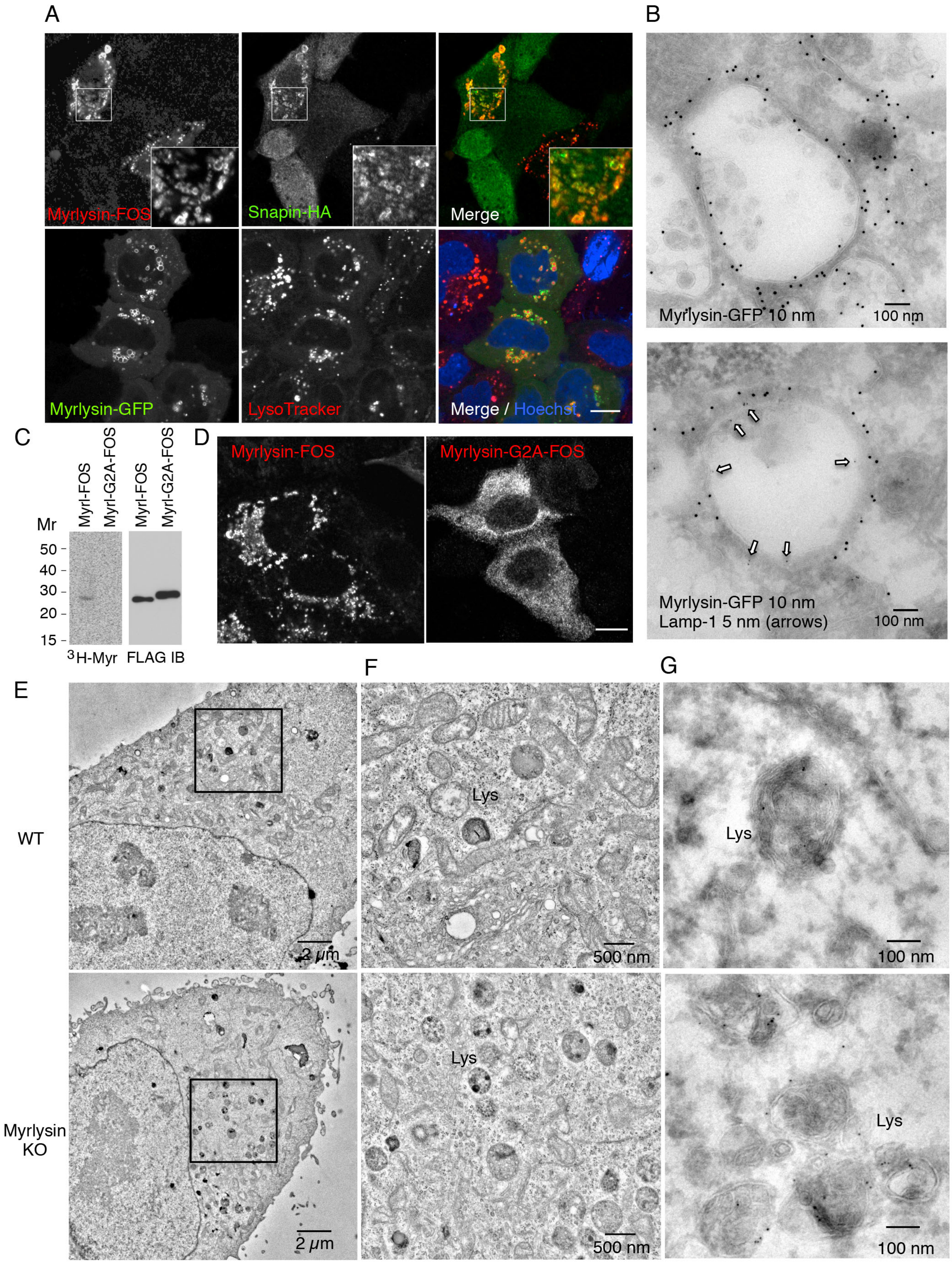

Pu et al.

Fig. S3

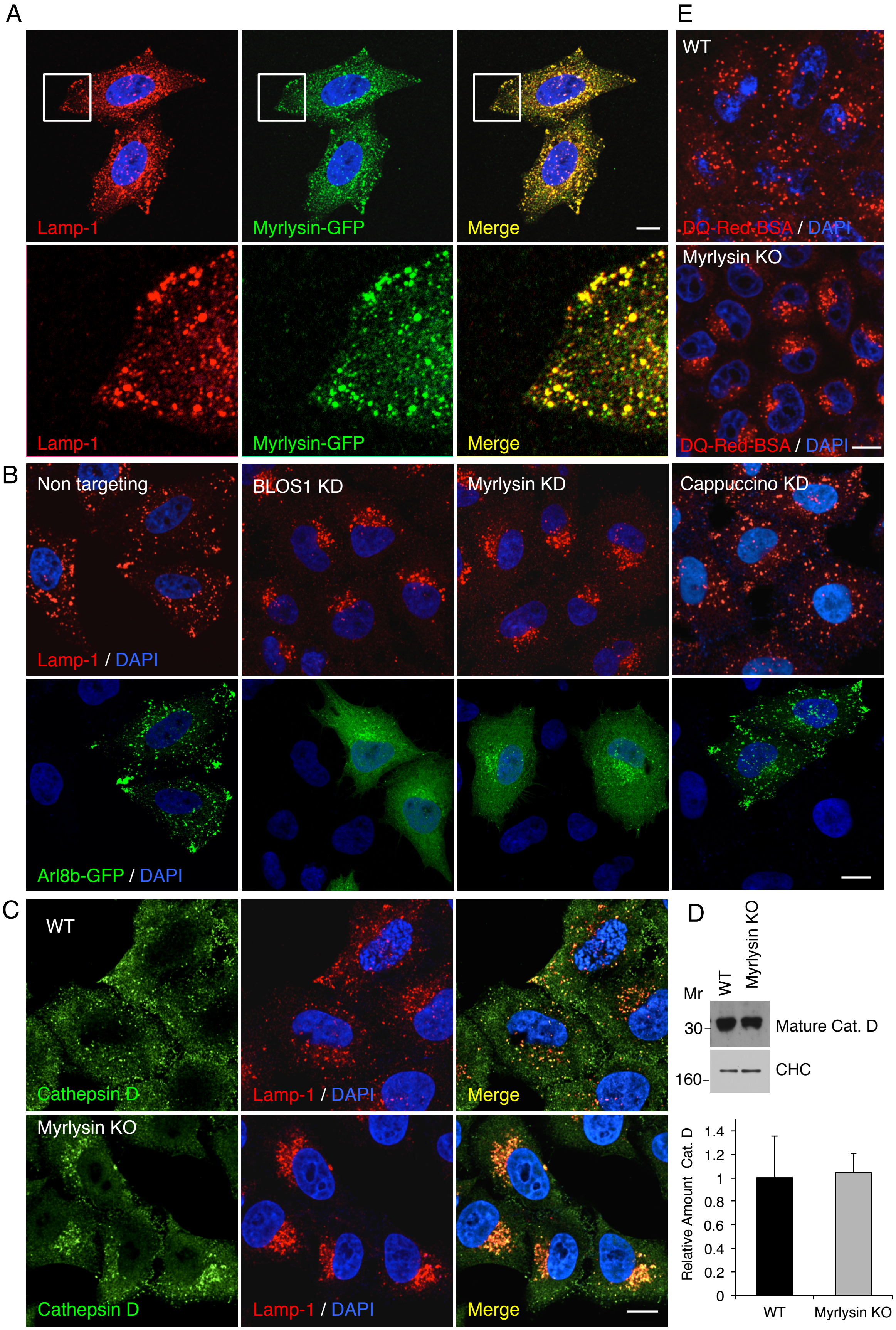

Pu et al.

Fig. S4

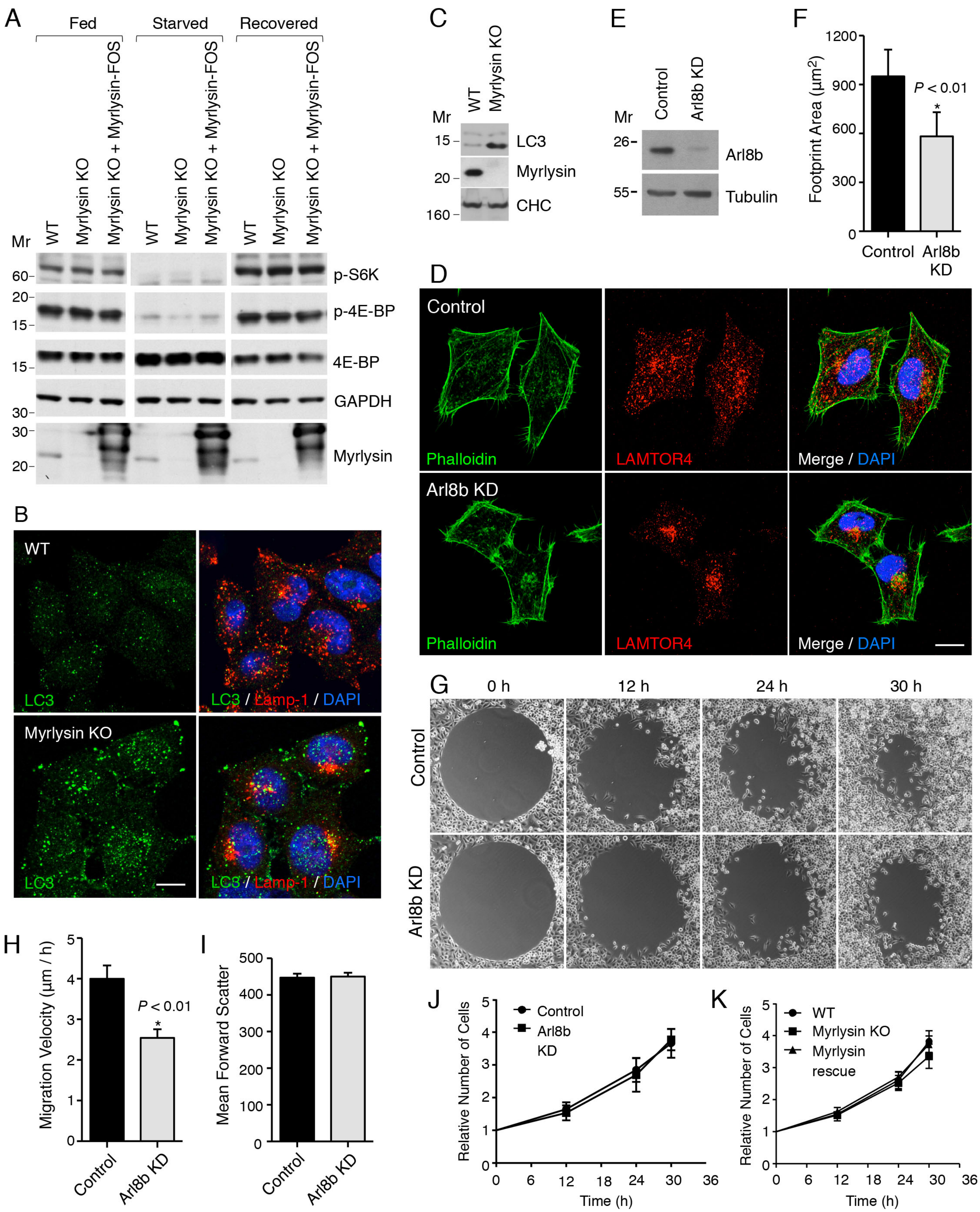

Pu et al.

SUPPLEMENTAL FIGURE LEGENDS

Fig. S1, related to Fig. 1. Properties of BORC subunits. (A) The program COILS (embnet.vital-it.ch/software/COILS_form.html) predicts the presence of coiled-coil regions in five subunits of BORC, as is the case for BLOC-1 subunits. Another program, MultiCoil (groups.csail.mit.edu/cb/multicoil/cgi-bin/multicoil.cgi), predicts that the coiled coils in all of these proteins, except for MEF2BNB, are trimeric. (B) Expression of Myrlysin in tissues from mouse and cell lines from different species. Mouse tissues and cell lines from various species were disrupted by sonication in 2x SDS-PAGE sample buffer, and proteins precipitated with 10% TCA. After washing with acetone, the pellets were dissolved in 2x SDS-PAGE sample buffer and equal amounts of total protein were analyzed by SDS-PAGE and immunoblotting (IB) with antibodies to LOH12CR1 (Myrlysin) and actin (control). The positions of molecular mass (Mr) markers (in kDa) are indicated. (C) Phylogenetic analysis of BORC subunit orthologs in members of different eukaryotic groups. Protein sequence homology searches were performed using the PSI-BLAST program with two iterations (Altschul et al., 1997). Top hits in the different species were confirmed by reverse PSI-BLAST of human sequences. Green indicates presence and red absence of orthologs. *Capsaspora owczarzaki*, *Rhizophagus irregularis* and *Acanthamoeba castellanii* are non-metazoans but contain orthologs of metazoan genes not found in other non-metazoans (Ruiz-Trillo et al., 2008; Barlow et al., 2014). The more sensitive HHpred tool (Soding et al., 2005) detected weak homology of LOH12CR1 to *S. cerevisiae* Snn1p (Ynl086wp; Snapin homolog) (significance value E=0.52) and C17orf59 to *S. cerevisiae* Cnl1p (Ydr357cp; Cappuccino homolog) (E=0.0054), both components of a yeast BLOC-1-like complex (Hayes et al., 2011; John Peter et al., 2013). Our analyses do not rule out the existence of more distantly related homologs in some of the negative (red) species.

Fig. S2, related to Fig. 3. Myristoylation-dependent association of Myrlysin with lysosomes and morphology of lysosomes in Myrlysin-KO cells. (A) Co-localization of Myrlysin with Snapin and LysoTracker. HeLa cells were transiently transfected with plasmids encoding the indicated proteins and analyzed by immunofluorescence microscopy for Myrlysin-FOS (using antibody to the FLAG tag) and Snapin-HA, or live-cell imaging for Myrlysin-GFP and LysoTracker. Scale bar: 10 μm. The inset shows a 2.5-fold magnification of the boxed area. (B) Immunoelectron microscopy of Myrlysin-GFP and Lamp-1. HeLa cells were transiently transfected with a plasmid encoding Myrlysin-GFP and analyzed by immunoelectron microscopy using antibodies to GFP and Lamp-1, followed by secondary antibodies conjugated to 10 nm (GFP) and 5 nm (Lamp-1, arrows) gold particles. (C) Metabolic labeling of Myrlysin with [^{3}H]-myristic acid. The Myristoylator program (Bologna et al., 2004) predicts that Myrlysin is N-terminally myristoylated in all species in which it is expressed. To test if human Myrlysin is myristoylated, HeLa cells were transfected with plasmids encoding Myrlysin-FOS or Myrlysin-G2A-FOS and metabolically labeled with [^{3}H]-myristic acid as described in Supplemental Experimental Procedures. Immunoprecipitates were analyzed by SDS-PAGE and phosphorimaging (for [^{3}H]-myristoylated Myrlysin) and immunoblotting (for total Myrlysin). Notice the labeling of Myrlysin-FOS but not Myrlysin-G2A-FOS with [^{3}H]-myristic acid. The positions of molecular mass (Mr) markers (in kDa) are indicated. Myrl: Myrlysin. Myr: myristic acid. (D) Immunofluorescent confocal microscopy of Myrlysin-FOS and Myrlysin-G2A-FOS expressed by transfection in HeLa cells and stained for the FLAG epitope. Notice the association of Myrlysin-FOS with lysosomes and the cytosolic distribution of Myrlysin-G2A-FOS. Scale bar: 10 μm. (E) Conventional electron microscopy showing that late endosomes and lysosomes are more clustered in the pericentriolar area but have normal morphology in Myrlysin-KO cells. (F) Magnified images of the boxed areas in E. Arrow points to a centriole. (G) Cryo-immunoelectron microscopy showing the appearance of lysosomes in WT and Myrlysin-KO cells labeled with antibody to Lamp-1 and secondary antibody conjugated to 6 nm gold particles. Lys: lysosome.

Fig. S3, related to Fig. 5. Properties of Myrlysin-KO cells. (A) Co-localization of Myrlysin-GFP stably expressed in Myrlysin-KO cells with Lamp-1. Scale bar: 10 μm. The lower row shows 4.5-fold-magnified views of the boxed areas. (B) KD of Myrlysin or BLOS1, but not Cappuccino, using siRNAs causes juxtanuclear clustering of lysosomes and dissociation of Arl8b into the cytosol in H4 human neuroglioma cells. Cells were treated twice with siRNAs to Myrlysin, BLOS1 or Cappuccino, or a non-targeting siRNA, as described in Experimental Procedures. Arl8b-GFP was expressed by transfection three days after the first siRNA treatment. Cells were fixed with 4% paraformaldehyde and stained for GFP, Lamp-1 and nuclear DNA (DAPI). Images were obtained by confocal microscopy. (C) WT and Myrlysin-KO cells were immunostained for the lysosomal protease Cathepsin D, Lamp-1 and nuclear DNA (DAPI). (D) WT and Myrlysin-KO cells were analyzed by SDS-PAGE and immunoblotting for Cathepsin D (Cat. D) and clathrin heavy chain (CHC) (control). The positions of molecular mass (Mr) markers (in kDa) are indicated (upper panel). Immunoblot results were quantified using ImageJ software from three independent experiments. The amounts of Cathepsin D in WT and Myrlysin-KO cell lysates were normalized to that of CHC and related to the amount of Cathepsin D in WT cells (arbitrarily defined as 1). Values are the mean ± SD (lower panel). (E) WT and Myrlysin-KO cells were incubated with DQ-Red BSA for 4 h, fixed with 4% paraformaldehyde, and imaged under a confocal microscope. Scale bars: 10 μm.

Fig. S4, related to Fig. 7. Effects of Myrlysin KO on mTORC1 signaling and LC3 levels, and of Arl8b KD on cell spreading and migration. (A) Myrlysin KO does not affect mTORC1 activity. WT, Myrlysin-KO, and Myrlysin-KO cells rescued with Myrlysin-FOS were kept in fresh DMEM with 10% FBS (fed), or HBSS buffer containing Ca^{2+} and Mg^{2+} for 2 h (starved), or treated with DMEM plus 10% FBS for 20 min after starvation (recovered). Cells were extracted and subjected to SDS-PAGE and immunoblotting using the indicated antibodies. The positions of molecular mass (M_r) markers (in kDa) are indicated. (B) WT and Myrlysin-KO cells were fixed with -20°C methanol and immunostained for LC3, Lamp-1 and nuclear DNA (DAPI). Images were obtained by confocal microscopy. Scale bar: 10 μm. (C) Cell lysates from WT and Myrlysin-KO cells were analyzed by immunoblotting with the indicated antibodies. The positions of molecular mass (Mr) markers (in kDa) are indicated. (D) Control and Arl8b-KD HeLa cells generated as described in Supplemental Experimental Procedures were stained with phalloidin-Alexa647, antibody to LAMTOR4 and DAPI, and imaged by confocal microscopy. Scale bar: 10 μm. (E) Arl8b-KD efficiency was evaluated by immunoblotting with antibodies to Arl8b and tubulin (control). The positions of molecular mass (Mr) markers (in kDa) are indicated. (F) The footprint area of control and Arl8b-KD cells was calculated using ImageJ from 100 phalloidin-stained cells in each group. Values are the mean ± SD. *P* values were calculated using Student's t-test. (G,H) Two-dimensional cell migration was analyzed using a circular gap closure assay. Images were captured at the indicated time points (G). The empty area was measured using ImageJ, and cell migration velocity calculated from the images at 0 and 24 h in three independent experiments. Values are the mean ± SD. *P* values were calculated using Student's t-test (H). (I) Control and Arl8b-KD cells were detached from culture plates using 20 mM EDTA in PBS, and forward scatter was analyzed by flow cytometry of 50,000 cells in each group. Error bars indicate coefficient of variation. (J) Growth curves of control and

Arl8b-KD cells. Cells were cultured on plates containing DMEM and 10% FBS for 24 h. Numbers of the cells at each time point were counted and related to the number of cells at time 0 (arbitrarily defined as 1). (K) Growth curves of WT, Myrlysin-KO and Myrlysin-GFP rescued HeLa cells analyzed as in J.

SUPPLEMENTAL TABLE LEGENDS

Table S1, related to Fig. 1. Mass spectrometry analysis of proteins that copurify with BLOS2. OSF-tagged BLOS2 stably expressed in HeLa cells was isolated by tandem affinity purification, and co-purifying proteins were analyzed by mass spectrometry as described in Experimental Procedures. The experiment was performed with two different clones of OSF-BLOS2-expressing clones. BLOC-1 subunits are highlighted in orange, AP-3 subunits in green, and Ragulator subunits in pink; another set of uncharacterized proteins (subsequently found to be BORC subunits) are highlighted in yellow. First column: number of unique peptides; second column: number of total peptides; third column: average of XCorr scores.

Table S2, related to Fig. 2. Mass spectrometry identification of bands from recombinant BORC purification. Recombinant BORC was produced in *E. coli* and analyzed by mass spectrometry as described in Experimental Procedures and Supplemental Experimental Procedures.

SUPPLEMENTAL MOVIE LEGEND

Movie S1, related to Fig. 6. Lysosome movement in WT and Myrlysin-KO cells. WT and Myrlysin-KO cells were seeded on fibronectin-coated Lab-Tek chambers (Thermo) and transfected with a plasmid encoding Lamp-1-GFP. Live-cell imaging was performed using a Zeiss LSM710 confocal microscope equipped with Definite Focus (Carl Zeiss) and an environmental chamber (Zeiss) set at 37°C and 5% CO_2. Images were captured with a 63x 1.4 oil objective over a period of 17 min at 1.9-s intervals.

SUPPLEMENTAL EXPERIMENTAL PROCEDURES

Purification and Mass Spectrometry of Recombinant BORC

A pST39 plasmid (Tan et al., 2005; Lee et al., 2012) encoding recombinant BORC (Fig. 2C) was expressed in pLys S competent cells (Agilent, Santa Clara, CA) cultured in 2x YT medium, induced with 1 mM isopropyl β-D-thiogalactopyranoside when A600 reached 0.6, and grown at 20°C for 14 h after induction. Cells were lysed by sonication in PBS with 1% Triton X-100 and a protease inhibitor cocktail (without EDTA) (Roche, Basel, Switzerland), and the supernatant was cleared by centrifugation at 10,000 *g* for 30 min. The cleared extract was sequentially bound to nickel-nitrilotriacetic acid (Ni-NTA) resin and glutathione resin (GE Healthcare, Buckinghamshire, UK) to isolate recombinant BORC. TEV protease was used to remove the 6His and GST tags.

Recombinant BORC was analyzed by size-exclusion chromatography on a Superose 6 column (GE Healthcare) in 0.05 M Tris-HCl pH 7.4, 0.3 M NaCl, 1 mM EDTA, 0.5% Tween 20 and 0.5 mM tris(2-carboxyethyl)phosphine (TCEP). Fractions (0.5 ml) were collected and subjected to SDS-PAGE, followed by Coomassie blue staining. Protein bands were excised from Coomassie Blue stained gels and digested with trypsin using standard protocols (Jiang et al., 2010). Sequencing grade trypsin (200 ng) (Promega Corp., Madison, WI) was added to each destained and dehydrated gel fragment; these were covered with 100 mM ammonium bicarbonate and incubated overnight at 37 ºC. The peptides were extracted, dried under vacuum, and reconstituted in 0.1% trifluoroacetic acid (TFA), followed by concentration and cleanup using C18 ZipTips (Millipore, Billerica, MA). The resulting peptides were analyzed by LC-ESI-MS/MS using an LCQ Deca ion trap mass spectrometer (ThermoFisher, Waltham, MA) equipped with an in-house packed reversed phase column (C18 – 75 μm ID x 5 cm, 5 μm particle size) fitted directly at the electrospray source. Tandem mass spectra were extracted using Bioworks version 3.3.1, and the extracted data files from each LC run were merged into a single MGF file for database searching. Charge state deconvolution and deisotoping were not performed. The spectra were analyzed using Mascot (Matrix Science, London, UK; version 2.4.0) and X! Tandem [thegpm.org; version CYCLONE (2010.12.01.1)], searching the mammalian subset of the Sprot_050113 database (66,254 entries). The digestion enzyme specificity was set for trypsin, with a parent ion tolerance of 1.2 Da and fragment ion mass tolerance of 0.6 Da. Oxidation of methionine was set as a variable modification. Scaffold (version Scaffold_3.3.2, Proteome Software Inc., Portland, OR) was used to validate MS/MS based peptide and protein identifications. Peptide identifications were accepted if they could be established at greater than 95.0% probability as specified by the Peptide Prophet (Keller et al., 2002). Protein probabilities were assigned using the Protein Prophet algorithm (Nesvizhskii et al., 2003), and protein identifications were accepted if they could be established at greater than 99.0% probability and contained at least two identified peptides.

Metabolic Labeling with [^{3}H]-Myristic Acid

HeLa cells transfected with plasmids encoding Myrlysin-FOS or Myrlysin-G2A-FOS were metabolically labeled with [^{3}H]-myristic acid as previously described (Jackson and Magee, 2001). Briefly, 24 h after transfection, cells were incubated in DMEM containing 5 mM sodium pyruvate for 1 h at 37°C, after which dialyzed FBS (Life Technologies, Grand Island, NY) loaded with [9,10(n)-^{3}H]-myristic acid (American Radiolabeled Chemicals, St. Louis, MO) was added to a concentration of 10% FBS and 50 μCi/ml [^{3}H]-myristic acid. After overnight labeling, Myrlysin-FOS and Myrlysin-G2A-FOS were pulled down with StrepTactin beads as described in Experimental Procedures and analyzed by SDS-PAGE. The tritium signal was detected by exposing the dried gel to a tritium screen (GE Healthcare) and scanning on a Typhoon phosphorimager.

Electron Microscopy

For conventional electron microscopy (EM), the samples were prepared as previously described (Neunuebel et al., 2012). In brief, cells grown on coverslips were fixed with 2% glutaraldehyde/2% formaldehyde in 0.1 M cacodylate buffer pH 7.2 followed by post-fixation in 1% osmium tetroxide. Upon dehydration and embedding in EMBed-812 (EM Science, Horsham, PA), the coverslips were removed by hydrofluoric acid, cells were thin-sectioned parallel to the glass, and sections were stained with uranyl acetate.

For EM immunocytochemistry, cells were prepared according to a modification of the Tokuyasu method (Tokuyasu, 1980). Cell pellets were fixed in 6% formaldehyde in PHEM (60 mM PIPES, 25 mM HEPES, 2 mM $MgCl_2$, 10 mM EGTA pH 6.9), embedded in gelatin, cryoprotected with 2.1 M sucrose in PHEM overnight, mounted on aluminum pins, and frozen in liquid nitrogen. Frozen sections (70-80 nm) were cut at -120°C on a Leica EM UC7 microtome with EM FC7 cryoadapter (Leica, Wetzlar, Germany), picked with a drop of 1:1 mixture of 2% methylcellulose and 2.1 M sucrose, and transferred to nickel grids coated with Formvar/carbon film. The sections were immunolabeled with primary antibody and the labeling was visualized using Aurion gold conjugates (Aurion, Wageningen, Netherlands). Eventually, the sections were contrasted and embedded in 2% methylcellulose, 0.2% uranyl acetate, and air-dried.

Samples were examined under a Tecnai 20 Biotwin TEM (FEI, Hillsboro, OR) at 120 kV accelerating voltage. The images were recorded by AMT XR-81 CCD camera (AMT, Woburn, MA).

Flow Cytometry

Confluent cells were detached from 12-well tissue culture plates by incubation with 20 mM EDTA in PBS and harvested by centrifugation for 5 min at 400 *g*. The cell pellets were resuspended in 500 μl PBS and filtered on cell strainers (Corning Inc., Corning, NY). Cells were on a FACSCalibur flow cytometer using CellQuest software (BD Biosciences, San Jose, CA).

Generation of Stably-transduced Arl8b Knock-down Cell Lines

A lentivirus-based shRNA system was purchased from Sigma (St. Louis, MO). Briefly, lentivirus particles were prepared by transfecting HEK293T cells with Arl8b shRNA plasmid or control shRNA plasmid and the lentivirus packaging plasmid. Forty-eight hours after transfection, supernatants were filtered through a 0.45 µm PVDF-filter to remove cell debris. HeLa cells were infected with the viruses and the stably transduced cells were selected with 2 µg/ml puromycin (Sigma). Knockdown efficiency was assessed by immunoblotting using antibody to Arl8b.

Other Methods

Immunoprecipitation (Bonifacino et al., 2001), SDS-PAGE (Gallagher, 2007) and immunoblotting (Gallagher et al., 2011) were performed as previously described.

Plasmids used in this study

Vector	Insert	Tag	Remarks
pCI-neo	Pallidin	N-3myc	
	Snapin	N-3myc	
	Snapin	N-3HA	
	Cappuccino	N-3myc	
	Muted	N-3myc	

	Dysbindin	N-3myc	
	BLOS1	N-13myc	
	BLOS3	N-3myc	
	KXD1	N-3myc	
	Dianomin (C10orf32)	N-3myc	
	MEF2BNB	N-3myc	
EGFP-N1	Myrlysin (LOH12CR1)	C-EGFP	
	Lamp-1	C-EGFP	
	Lamp-1-KBS	C-EGFP	
EGFP-C1	KIF5A	N-EGFP	
	Rab7	N-EGFP	
pcDNA3.1	Myrlysin (LOH12CR1)	N-OSF; C-FOS	
	BLOS2	N-OSF	
	Lyspersin (C17orf50)	N-OSF; C-FOS	
pQCXIP	KLC2	C-GFP	
pcDNA3.1/CT-GFP	Arl8b	C-GFP	Gift from Dr. J. H. Brumell
pCMV-myc	SKIP	N-myc	Gift from Dr. S. Méresse

Antibodies used in this study

Antigen	Source	Cat. Number
Cathepsin D	Calbiochem	219361

CD63	BD Biosciences	556019
CHC	Santa Cruz	sc-6579
p-4E-BP1 (Thr37/46)	Cell Signaling Technology	2855
4E-BP1	Cell Signaling Technology	9452
FLAG epitope	Sigma-Aldrich	F1804
GFP	Life Technology	A11122
GFP-HRP	Miltenyi Biotec Inc.	130-091-833
HA epitope	Covance	MMS-101P
Lamp-1	Abcam	ab25630
LAMTOR4	Cell Signaling Technology	13140
LC3B	Cell Signaling Technology	3868
Myc epitope	Cell Signaling Technology	2276
Myc-HRP	Santa Cruz	sc-40 HRP
Myrlysin (LOH12CR1)	Abgent	AP5806b
Myrlysin (LOH12CR1)	Proteintech	17169-1-AP
Pallidin	Gift from Dr. E. Dell'Angelica	
Pallidin	Proteintech	10891-2-AP
p-S6 Kinase (Thr389)	Cell Signaling Technology	9234
Snapin	SYSY	148 002
TfR	Santa Cruz	sc-376278

SUPPLEMENTAL REFERENCES

Altschul, S. F., Madden, T. L., Schaffer, A. A., Zhang, J., Zhang, Z., Miller, W., and Lipman, D. J. (1997). Gapped BLAST and PSI-BLAST: a new generation of protein database search programs. Nucleic Acids Res *25*, 3389-3402.

Barlow, L. D., Dacks, J. B., and Wideman, J. G. (2014). From all to (nearly) none: Tracing adaptin evolution in Fungi. Cell Logist *4*, e28114.

Bologna, G., Yvon, C., Duvaud, S., and Veuthey, A. L. (2004). N-Terminal myristoylation predictions by ensembles of neural networks. Proteomics *4*, 1626-1632.

Bonifacino, J. S., Dell'Angelica, E. C., and Springer, T. A. (2001). Immunoprecipitation. Curr Protoc Immunol *Chapter 8*, Unit 8.3.

Gallagher, S., Winston, S. E., Fuller, S. A., and Hurrell, J. G. (2011). Immunoblotting and immunodetection. Curr Protoc Cell Biol *Chapter 6*, Unit6.2.

Gallagher, S. R. (2007). One-dimensional SDS gel electrophoresis of proteins. Curr Protoc Cell Biol *Chapter 6*, Unit 6.1.

Hayes, M. J., Bryon, K., Satkurunathan, J., and Levine, T. P. (2011). Yeast homologues of three BLOC-1 subunits highlight KxDL proteins as conserved interactors of BLOC-1. Traffic *12*, 260-268.

Jackson, C. S., and Magee, A. I. (2001). Metabolic labeling with fatty acids. Curr Protoc Cell Biol *Chapter 7*, Unit 7.4.

Jiang, X. S., Backlund, P. S., Wassif, C. A., Yergey, A. L., and Porter, F. D. (2010). Quantitative proteomics analysis of inborn errors of cholesterol synthesis: identification of altered metabolic pathways in DHCR7 and SC5D deficiency. Mol Cell Proteomics *9*, 1461-1475.

John Peter, A. T., Lachmann, J., Rana, M., Bunge, M., Cabrera, M., and Ungermann, C. (2013). The BLOC-1 complex promotes endosomal maturation by recruiting the Rab5 GTPase-activating protein Msb3. J Cell Biol *201*, 97-111.

Keller, A., Nesvizhskii, A. I., Kolker, E., and Aebersold, R. (2002). Empirical statistical model to estimate the accuracy of peptide identifications made by MS/MS and database search. Anal Chem *74*, 5383-5392.

Lee, H. H., Nemecek, D., Schindler, C., Smith, W. J., Ghirlando, R., Steven, A. C., Bonifacino, J. S., and Hurley, J. H. (2012). Assembly and architecture of biogenesis of lysosome-related organelles complex-1 (BLOC-1). J Biol Chem *287*, 5882-5890.

Nesvizhskii, A. I., Keller, A., Kolker, E., and Aebersold, R. (2003). A statistical model for identifying proteins by tandem mass spectrometry. Anal Chem *75*, 4646-4658.

Neunuebel, M. R., Mohammadi, S., Jarnik, M., and Machner, M. P. (2012). Legionella pneumophila LidA affects nucleotide binding and activity of the host GTPase Rab1. J Bacteriol *194*, 1389-1400.

Ruiz-Trillo, I., Roger, A. J., Burger, G., Gray, M. W., and Lang, B. F. (2008). A phylogenomic investigation into the origin of metazoa. Mol Biol Evol *25*, 664-672.

Soding, J., Biegert, A., and Lupas, A. N. (2005). The HHpred interactive server for protein homology detection and structure prediction. Nucleic Acids Res *33*, W244-8.

Tan, S., Kern, R. C., and Selleck, W. (2005). The pST44 polycistronic expression system for producing protein complexes in Escherichia coli. Protein Expr Purif *40*, 385-395.

Tokuyasu, K. T. (1980). Immunochemistry on ultrathin frozen sections. Histochem J *12*, 381-403.